communications biology

A Nature Portfolio journal

Article

https://doi.org/10.1038/s42003-025-07884-5

The *Escherichia coli* AZY operon links copper uptake to antibiotic resistance

Caitlin D. Palmer[1,3], Yara Ghnamah[2,3], Nurit Livnat-Levanon[2], Oded Lewinson[2] ✉ & Amy C. Rosenzweig[1] ✉

Copper import to the bacterial cytoplasm has been underinvestigated as bacterial cuproenzymes are extracytoplasmic. However, copper must access the cytoplasm to interact with metal-dependent transcription factors. In particular, the multiple drug antibiotic resistance (*mar*) operon is induced by a copper signal, the source of which has not been established. Here we show that the *Escherichia coli* AZY operon, which encodes the copper-binding periplasmic proteins YobA and YebY and the putative copper importer YebZ, mediates copper uptake. Copper uptake by YebZ depends on two conserved histidine residues and is modulated by YobA and YebY. Moreover, the AZY proteins are necessary for activation of the *mar* operon and mediate resistance to multiple antibiotics in a copper-dependent fashion. AZY-like operons are widespread in gram-negative bacteria, suggesting that this previously unknown link between copper and antibiotic resistance is a general mechanism that may offer an alternative therapeutic target for multidrug resistance.

Copper is an essential metal ion that cycles between the Cu^{+} and Cu^{2+} states to facilitate redox chemistry in biochemical processes central to all kingdoms of life[1,2]. However, excess copper is toxic, leading to oxidative damage through Fenton-like chemistry, disruption of iron/sulfur clusters, interference with signaling pathways, and cuprotosis[3–5]. As such, copper homeostasis involves a complex web of transporters, chaperones, and regulatory proteins that regulate copper levels to ensure cuproprotein function without deleterious effects[6,7]. Eukaryotic copper distribution involves copper translocation in and out of different cellular compartments, whereas prokaryotic copper handling requires transport across the outer and inner membranes[8].

In gram-positive bacteria, cuproenzymes are embedded in the cellular membrane and thus can obtain copper directly from the environment[9]. By contrast, copper enters the periplasm of gram-negative bacteria through porins[9] or chalkophore uptake systems[10]. While export and copper trafficking in the periplasm of gram-negative bacteria have been studied extensively, mechanisms for copper import into the cytoplasm remain underinvestigated because bacterial cuproenzymes are localized to the periplasm and inner membrane[11]. One exception is copper delivery to some extracytoplasmic cuproenzymes by P_{1B}-ATPases located in the inner membrane. In these cases, which include loading of cytochrome *c* oxidase and periplasmic Cu,Zn superoxide dismutase, cytoplasmic copper is exported back to the periplasm by CopA2/CcoI[12,13] and GolT or CopA[14], respectively. The corresponding importers, CcoA[15] and CulT[16], are members of the major facilitator superfamily (MFS). A second exception is copper delivery to transcription factors in the cytoplasm. In *Escherichia coli*, copper binding by the regulator CueR switches it from a repressor to an activator of expression of the CopA efflux pump[17]. Another copper-responsive regulator in *E. coli* is MarR, which represses expression of the multiple antibiotic resistance (*mar*) operon[18,19]. In the presence of inducers such as salicylate, norfloxacin, and ampicillin, intracellular copper levels increase and copper-mediated oxidation of a MarR cysteine residue leads to its dissociation from DNA[20]. Once MarR dissociates, the activator MarA is expressed and upregulates drug efflux pumps, DNA repair genes, and other resistance mechanisms, leading to multiple antibiotic resistance[21,22]. While the increase in cytoplasmic copper has been attributed to oxidative damage by inducers and release from copper-containing membrane proteins such as NADH:quinone oxidoreductase (NDH-2)[20], it is also possible that copper is imported by an inner membrane transporter.

A possible candidate for this importer is YebZ, encoded in the *E. coli* AZY operon[23]. YebZ belongs to the CopD family[24], members of which typically have 8 predicted transmembrane helices (TMHs). Present in the genomes of numerous bacteria, genes encoding these proteins are usually found either paired with a gene encoding the periplasmic copper-binding protein CopC or as a CopCD fusion protein, as is the case for *Bacillus subtilis* YcnJ, which has been linked to copper uptake by genetic disruption experiments[25,26]. CopC and CopD have also been associated with copper accumulation in *Pseudomonas* species[27,28] and in methanotrophic bacteria[29]. In addition to YebZ, the AZY operon encodes a CopC homolog, YobA, which binds Cu^{2+} with high affinity[23], and a member of the DUF2251 family

[1]Departments of Molecular Biosciences and Chemistry, Northwestern University, Evanston, IL, USA. [2]Department of Biochemistry and the Rappaport Institute for Medical Sciences, Faculty of Medicine, The Technion-Israel Institute of Technology, Haifa, Israel. [3]These authors contributed equally: Caitlin D. Palmer, Yara Ghnamah. ✉e-mail: lewinson@technion.ac.il; amyr@northwestern.edu

denoted YebY. YebY structurally resembles the lantibiotic self-resistance protein MlbQ[30] and binds Cu^{+} and Cu^{2+} with low affinity[23]. In previous genetic studies, we showed that the AZY operon is not involved in copper tolerance or antioxidant defense, but might instead provide copper for membrane-bound proteins[23]. On the basis of the similarity of YebY to MlbQ and the known connection between copper and the *mar* operon[20], we also speculated that the AZY operon might play a role in antibiotic resistance[23].

Here we demonstrate that the AZY operon is indeed a copper uptake system, pinpoint specific YebZ residues associated with copper uptake, and probe the functions of YobA and YebY. Furthermore, we show that the AZY proteins are involved in the activation of the *mar* operon via copper acquisition, and that their removal leads to diminished multidrug resistance. Finally, a comprehensive bioinformatics analysis of the CopD family suggests that this mechanism of copper import for antibiotic resistance is likely widespread. These combined findings provide evidence for copper import into the bacterial cytoplasm, identify the specific transport system, and establish a link between copper import and antibiotic resistance pathways in bacteria.

Results

The AZY proteins modulate copper levels in *E. coli*

To test whether the AZY operon is involved in copper import, we first employed a reporter gene approach, fusing the genes of the *lux* operon (*luxCDABE*) downstream of the *copA* promoter, generating the plasmid $_{p}$*copA-Lux*. In *E. coli*, increased intracellular copper is sensed by CueR, which binds to the *copA* promoter and regulates the expression of the CopA efflux pump[31]. Wild-type (WT) *E. coli* (strain BW25113) were transformed with plasmid $_{p}$*copA-Lux* or with a control plasmid lacking a promotor upstream of the *lux* operon. Cells were then grown in an automated plate reader and at the onset of exponential growth, 50 μM $CuSO_4$ was injected into the growth media. Following $CuSO_4$ addition, a rapid increase in luminescence is observed for the $_{p}$*copA-Lux* cells, but not for the control cells expressing the promoter-less *lux* operon (Supplementary Fig. 1a). When water or $ZnSO_4$ was added instead of $CuSO_4$, the response of both cell types was minimal (Supplementary Fig. 1a). We conducted similar experiments with the *E. coli* mutant strain GG44, which lacks CopA and rapidly overaccumulates copper[32]. Indeed, upon $CuSO_4$ addition, the increase in luminescence was 30–40-fold higher in GG44 cells than in the isogenic parental WT strain (Supplementary Fig. 1b). These results indicate that the $_{p}$*copA-Lux* reporter can be used to specifically monitor copper influx into bacterial cells.

We then compared the intracellular copper contents of cells with the entire AZY operon deleted (Δ*AZY*) and cells of the isogenic parental WT strain, both transformed with plasmid $_{p}$*copA-Lux*. In the absence of added copper, the luminescence of WT and Δ*AZY* cells expressing $_{p}$*copA-Lux* was low and comparable (Fig. 1a). Upon injection of 50 μM $CuSO_4$, a rapid increase in the luminescence was observed for both cell types, but was 3–4-fold

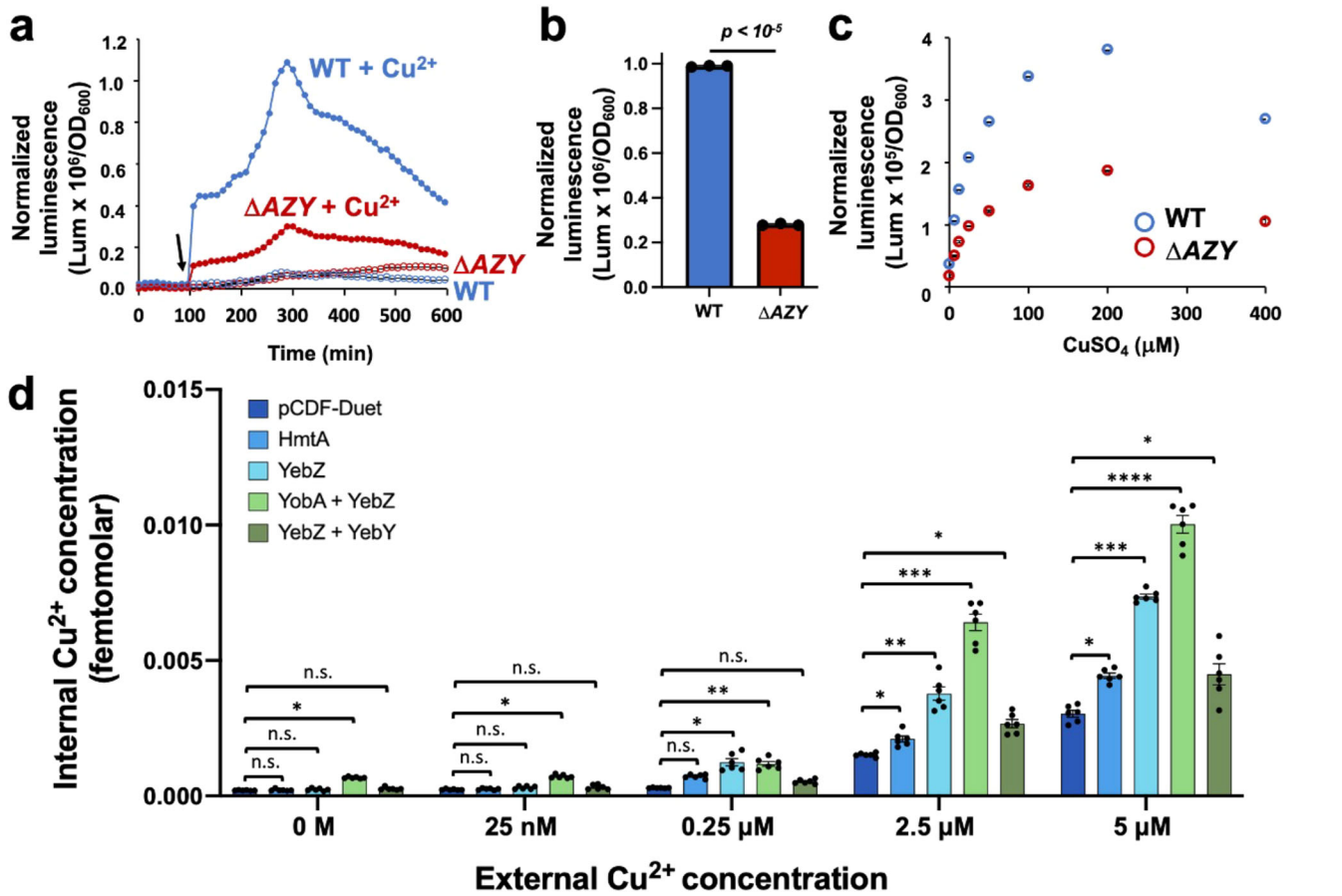

Fig. 1 | The AZY proteins are involved in copper import. a WT and Δ*AZY* cells (blue and red curves, respectively) expressing the luciferase reporter gene fused to the *copA* promoter were cultured in M9 minimal media, and at the time indicated by the arrow, 50 μM $CuSO_4$ (filled circles) or an equivalent volume of H_2O (open circles) was added. **b** Normalized luminescence of WT and Δ*AZY* cells (blue and red bars, respectively) expressing the luciferase reporter gene fused to the *copA* promoter at mid-exponential phase (5–6 h of growth). Also shown is the p value determined by a student's t-test. **c** Normalized luminescence of WT and Δ*AZY* cells (blue and red symbols, respectively) expressing the luciferase reporter gene fused to the *copA* promoter at mid-exponential phase (5–6 h of growth), cultured in the absence or presence of the indicated concentrations of $CuSO_4$. Results (**a**–**c**) are means of biological triplicates, and the error bars (shown inside of the open circles; some are smaller than icons) represent the standard deviations of the mean. **d** Copper content of *E. coli* C41(DE3) cells overexpressing a pCDF-Duet control plasmid, the known copper importer HmtA, YebZ, and dual combinations of YebZ and either YebY or YobA. Non-significant differences ($p > 0.05$) between the pCDF-Duet expressing cells and the other samples, as determined by one-way ANOVA (the Tukey-Kramer test), are marked "n.s." Significance values are noted as follows: *$p < 0.05$; **$p < 0.001$; ***$p < 0.0001$; ****$p < 0.00001$.

higher in WT cells (Fig. 1a, b). We then repeated these experiments using $CuSO_4$ concentrations of 5–400 μM. Importantly, the WT and Δ*AZY* strains exhibited identical growth behavior over this concentration range (Supplementary Fig. 2). At all concentrations, during both the lag (Supplementary Fig. 1c) and log (Fig. 1c) phases of growth, WT cells exhibited significantly higher luminescence than the Δ*AZY* cells. In contrast, single deletions of *yobA*, *yebZ*, and *yebY* did not affect the luminescence (Supplementary Fig. 3). These combined results suggest that YobA, YebZ, and YebY are involved in copper regulatory pathways, and likely function in concert.

To determine whether the transmembrane protein YebZ is the copper importer, full-length YebZ was overexpressed in *E. coli* C41(DE3) cells in the presence of 0–5 μM $CuSO_4$. The cellular copper content was then compared to that of C41(DE3) cells not overexpressing YebZ, as well as cells expressing the previously characterized copper-transporting P_{1B}-ATPase HmtA[32] (Fig. 1d, Supplementary Fig. 4). As compared to C41(DE3) cells alone or those transformed with empty vectors, the YebZ-overexpressing cells exhibited significantly higher levels of copper ($p < 0.0001$) (Fig. 1d, Supplementary Fig. 4). This effect was independent of the presence of a His_6 affinity tag, and no import was observed in the absence of glucose (Supplementary Fig. 4), implying that copper import by YebZ is an energy-dependent process. Notably, overexpression of YebZ led to an ~2.5x higher copper accumulation (Fig. 1d, 2.5–5 μM Cu^{2+}) than overexpression of HmtA[32]. While copper is provided as Cu^{2+} in these experiments, it could be reduced to Cu^{+} in the cell, precluding assignment of the oxidation state during import. Finally, YebZ-overexpressing cells were also treated with $ZnCl_2$, $FeSO_4$, and $CoCl_2$ under the same conditions to assess the specificity of the observed metal uptake (Supplementary Fig. 5). No significant increase in concentrations of these metal ions was observed, consistent with YebZ importing copper specifically.

To probe the functions of YobA and YebY, we overexpressed different combinations of the operon proteins and performed additional in vivo copper uptake experiments. Overexpression of YebZ and YobA in C41(DE3) cells showed a dramatic increase in the basal levels of copper, suggesting that the two proteins together can acquire copper from rich media more effectively than YebZ alone. After addition of 25 nM–5 μM Cu^{2+}, up to ~2–3 fold higher intracellular copper content was measured for these cells as compared to cells transformed with the corresponding empty vector (Fig. 1d, 2.5–5 μM Cu^{2+}). This highly significant ($p < 0.0001$) increase in copper content over the range of 0–5 μM Cu^{2+}, as compared to that observed with overexpression of YebZ alone, supports a key role for YobA in copper transport. Conversely, coexpression of YebZ with YebY decreases the amount of accumulated copper within the cell (Fig. 1d), suggesting that YebY might negatively regulate copper import and may have a competing role with YobA. At higher copper concentrations (≥ 12.5 μM Cu^{2+}, Supplementary Fig. 6a), this increase in intracellular content is not observed for YebZ or YebZ coexpressed with YobA or YebY, suggesting that at higher concentrations, copper likely enters the cell through other less specific pathways. Neither YobA nor YebY alone was sufficient to yield increased copper content (Supplementary Fig. 6b), supporting the assignment of YebZ as a copper importer.

To begin elucidating the molecular basis for specific copper uptake by YebZ, we generated a structural model using AlphaFold Multimer[33] (Fig. 2a). In the model, two very highly conserved histidine residues, His 135 and His 154, reside near the predicted periplasmic side of YebZ. These two histidines are present in 99% of unique CopD family member sequences that contain 8 TMHs (Fig. 2b). Modeling with AlphaFold Multimer[33] places the predicted copper binding site of YobA[23] within 5 Å of YebZ His 135 (Fig. 2a). Given that YobA binds copper[23] and that some members of the CopD family include a fused N-terminal CopC/YobA domain, these histidines might play a role in receiving copper from YobA. To assess their potential importance, we replaced His135 and His154 individually with alanine and repeated the uptake experiments. Expression of the H135A variant in *E. coli* C41(DE3) cells reduced the copper content significantly compared to that of cells overexpressing WT YebZ ($p < 0.01$) while expression of the H154A variant completely abolished copper uptake ability (p = n.s.) (Fig. 2c). Both variants were expressed at a similar level as WT YebZ (Supplementary Fig. 7). Thus, these two conserved histidine residues are critical for copper import.

The AZY proteins play a role in *mar*-mediated antibiotic resistance

Having established that the AZY operon proteins function in copper uptake, we next investigated the possibility that they are involved in activation of the

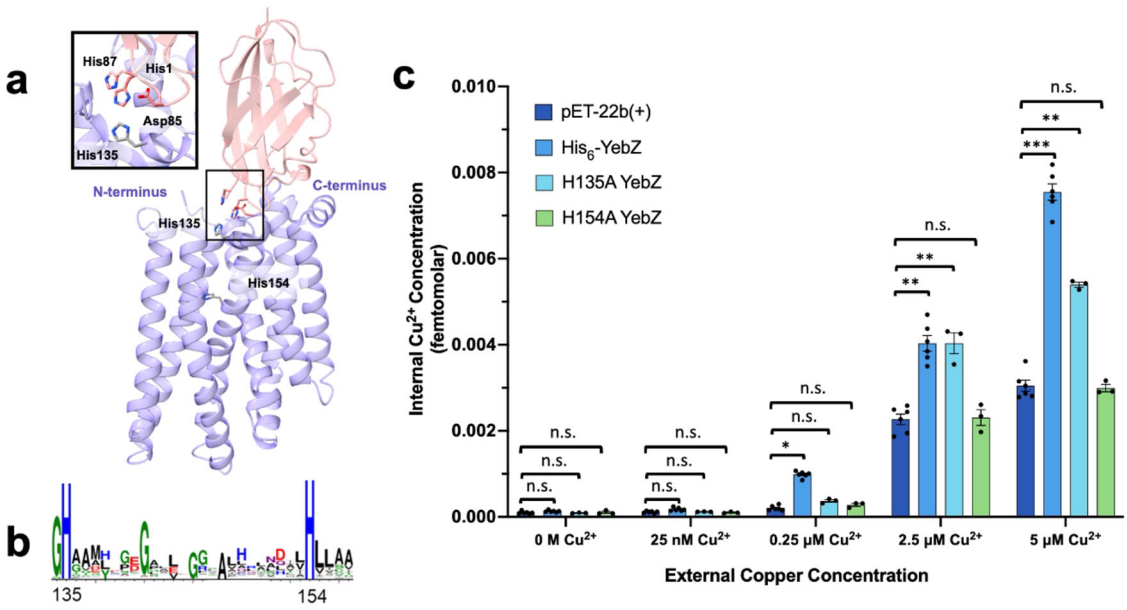

Fig. 2 | YebZ is a copper importer. a AlphaFold multimer model of the proposed YebZ (purple)-YobA (pink) interaction, with strictly conserved YebZ residue H135 and the proposed YobA Cu^{2+} copper-binding site shown as sticks and enlarged on the left. **b** Condensed sequence logo showing that His135 and His154 are strictly conserved in all CopDs with ≥ 8 TMHs (~ 3800 sequences). **c** Copper content of *E. coli* C41(DE3) cells transformed with the pET-22b(+) vector and cells expressing His_6-YebZ, His_6-H135A YebZ, and His_6-H154A YebZ. Each experiment includes at least $n \geq 3$ biological replicates. Non-significant differences ($p > 0.05$) between the C41(DE3) cells expressing the background expression vector and the other samples, as determined by one-way ANOVA (the Tukey-Kramer test), are marked "n.s." Significance values are noted as follows: *$p < 0.05$; **$p < 0.01$; and ***$p < 0.0001$.

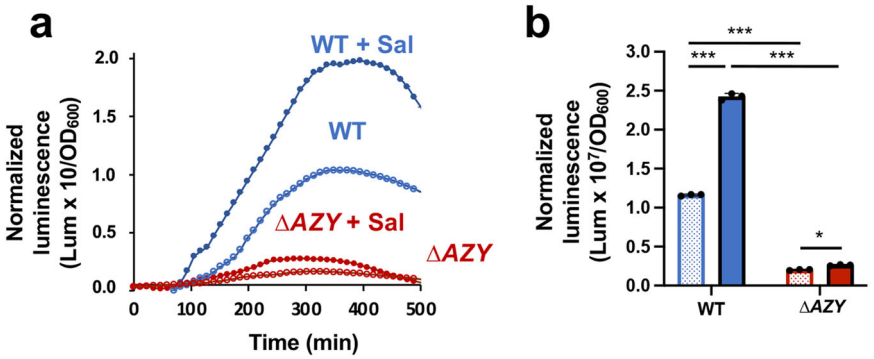

Fig. 3 | The AZY proteins are essential for activation of the *mar* pathway. a Cultures of WT and Δ*AZY* cells (blue and red curves, respectively) expressing the luciferase reporter gene fused to the *mar* operator were cultured in the absence or presence (open and filled circles, respectively) of the *mar* pathway inducer salicylic acid (2.5 mM). Shown are the averages of biological triplicates, and the error bars (shown unless smaller than icons) represent the standard deviations of the mean. **b** Normalized luminescence of WT and Δ*AZY* cells (blue and red bars, respectively) expressing the luciferase reporter gene fused to the *mar* operator at mid-exponential phase (5–6 h of growth), in the absence (open bars) or presence (filled bars) of the *mar* operator inducer salicylic acid (2.5 mM). Significance was determined using a one-way ANOVA test with a = 0.05 and p values (*** = $p < 10^{-13}$, * = $p < 0.05$). Each experiment shows the means of biological triplicates, and the error bars (shown unless smaller than icons) represent the standard deviations of the mean.

mar pathway. We again applied the reporter gene approach, this time fusing the *luxCDABE* genes downstream of the 5'UTR operator region of the *mar* operon to generate plasmid $_p$*marO-Lux*. We then measured the $_p$*marO-Lux* luminescence in the WT and Δ*AZY* strains, both in the absence and presence of salicylic acid, a known inducer of the *mar* pathway[34]. Under both constitutive and induced regimes, the luminescence decreased by 80–90% in the Δ*AZY* strain (Fig. 3a, b), suggesting that the AZY proteins are essential for the activation of the *mar* operon.

Since cells lacking the AZY proteins have diminished copper import capacity (Fig. 1a–c) and reduced activation of the *mar* operon (Fig. 3a, b), we hypothesized that Δ*AZY* cells would be more susceptible to antibiotics than WT *E. coli*. Before assessing antibiotic resistance, we assessed the fitness of the Δ*AZY* strain by culturing the cells in rich and minimal media, in the absence or presence of stressors unrelated to the *mar* pathway, including ethanol, SDS, and sodium cholate (Supplementary Fig. 8). Under all conditions, the growth of the WT and Δ*AZY* cells was similar, suggesting that deletion of the *AZY* genes does not pleiotropically compromise bacterial fitness.

We next tested the antibiotics tetracycline and chloramphenicol, which target the 30S and 50S subunits of the ribosome, respectively. Since resistance to tetracycline and chloramphenicol was shown to be independent of copper activation of the *mar* pathway[20], we reasoned that WT and Δ*AZY* cells would be equally susceptible to these two antibiotics, as was indeed the case (Fig. 4b, c). We then tested three additional antibiotics: norfloxacin, a quinolone that impairs bacterial DNA replication by inhibiting DNA gyrase; ciprofloxacin, a second-generation fluoroquinolone that inhibits both DNA gyrase and topoisomerase IV[35]; and ampicillin, a classical β-lactam that inhibits cell wall synthesis[36]. Resistance to these three antibiotics was previously reported to depend on copper activation of the *mar* pathway, and we selected concentrations of each at which the *mar* pathway is known to confer resistance[20,22] (Supplementary Fig. 9). As shown in Fig. 4d–f, the Δ*AZY* cells were significantly more susceptible to these *mar*-related antibiotics than the WT cells. After normal growth during the lag and early exponential phases, rapid bacterial killing and lysis occurred, resulting in a sudden drop in optical density. This pattern of initial growth followed by rapid killing is consistent with the known bactericidal effects of these antibiotics[37,38]. Taken together, these results indicate that the AZY operon is specifically involved in *mar* pathway-mediated multidrug resistance.

The AZY proteins link copper import to multiple antibiotic resistance

The results presented thus far demonstrate that YebZ functions as a copper importer, the activity of which is enhanced by the periplasmic protein YobA and diminished by the periplasmic protein YebY. In addition, we observed that the AZY proteins are essential for activation of the *mar* operon and for resistance to several antibiotics. We next hypothesized that if the AZY operon is indeed the crucial link connecting intracellular copper delivery to antibiotic resistance, then removing copper should have a detrimental effect on activation of the *mar* operon and antibiotic resistance in WT cells, but little to no effect in the Δ*AZY* strain. To test this, residual copper was removed from the buffers and growth media by the addition of the copper chelator triethylenetetramine (TETA)[20]. In support of the hypothesis, copper removal resulted in greatly reduced *mar* operon activity in WT cells (Fig. 5a), but had no effect in Δ*AZY* cells (Supplementary Fig. 10). Similarly, copper chelation by TETA increased the susceptibility of WT cells to norfloxacin by roughly 3-fold, while having almost no effect on the antibiotic susceptibility of Δ*AZY* cells (Fig. 5b). This finding strongly suggests that copper imported by the AZY system is involved in *mar* regulation and antibiotic resistance.

Copper import for antibiotic resistance may be a conserved mechanism in bacteria

To assess whether the link between copper import by the AZY proteins and antibiotic resistance could be widespread in gram-negative bacteria, an extensive bioinformatics analysis was performed using ~50,000 CopD family (pfam05425) sequences in the proteobacteria phylum from the Joint Genome Institute/Integrated Microbial Genomes (JGI/IMG) database. Most CopD family members are found in *Gammaproteobacteria* (Fig. 6a), primarily within the *Enterobacteriaceae* family. The sequences range in length from "truncated" CopDs predicted to have < 5 TMHs to sequences with multiple soluble domains or up to 12 TMHs (Fig. 6b). *E. coli* K12 YebZ falls within the largest cluster of sequences, suggesting that it is a good representative of gammaproteobacterial CopD homologs and the broader pfam05425 family. Approximately 50% of the sequences have 8 predicted TMHs and two highly conserved histidine residues corresponding to those implicated in YebZ function (Figs. 2, 6c). The truncated CopDs, which contain only the core four helix-bundle located at the N-terminus of the 8 TMH proteins, comprise ~35% of the sequences. Notably, only the first of the two conserved histidine residues is present in these truncated sequences (Fig. 6c). Most of the remaining sequences (~ 9%) include an N-terminal CopC domain, similar to *B. subtilis* YcnJ[25] (not included in this SSN as *B. subtilis* is gram positive), consistent with the increased copper uptake observed upon overexpression of YebZ together with YobA (Fig. 1d). Many of these multidomain CopCD sequences also contain a C-terminal DUF1775 domain (annotated YtkA or YcnI-like), and a small percentage of sequences

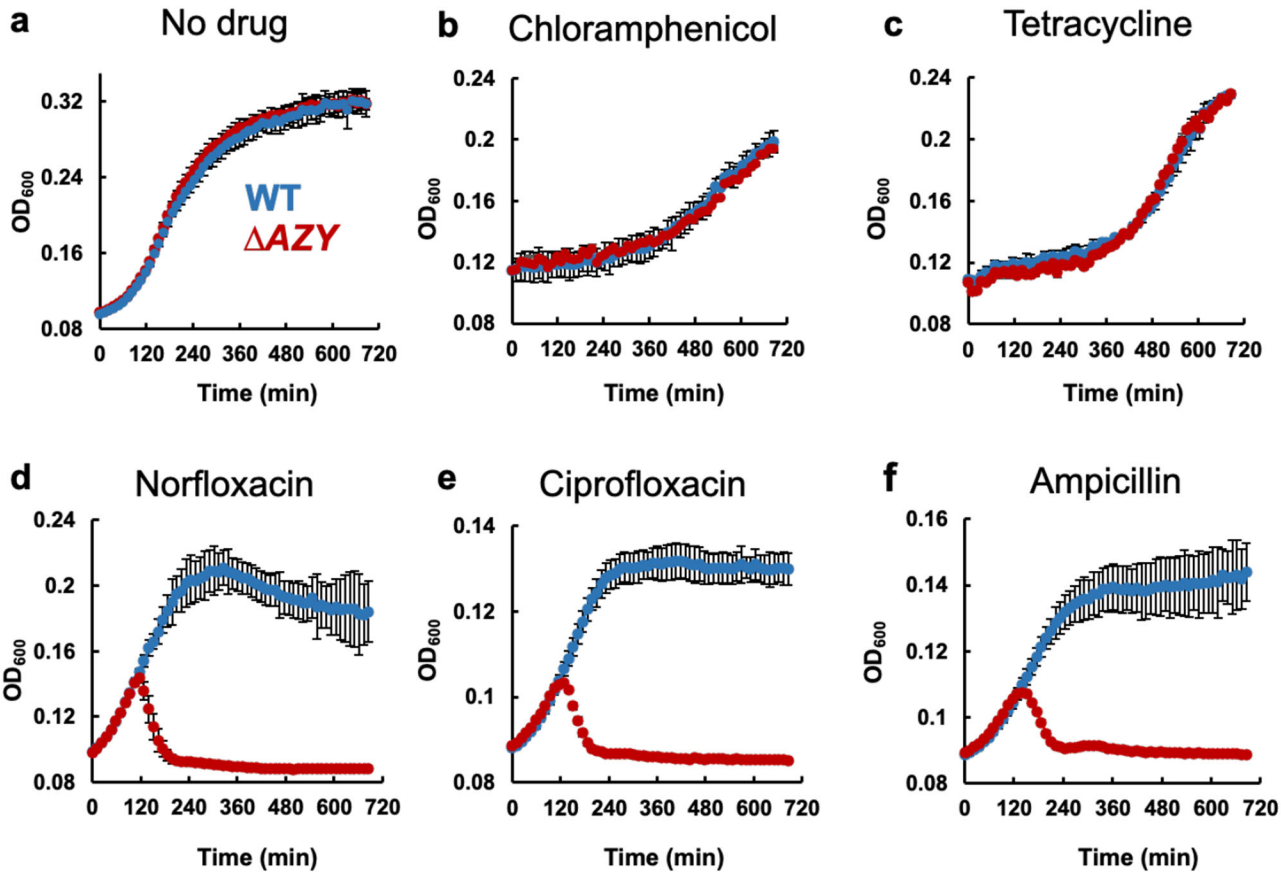

Fig. 4 | The AZY proteins are involved in multiple antibiotic resistance. Cultures of WT and Δ*AZY* cells (blue and red curves, respectively) were grown in M9 minimal media in the (**a**) absence or the presence of (**b**) 850 ng/mL chloramphenicol, (**c**) 175 ng/mL tetracycline, (**d**) 62.5 ng/ml norfloxacin, (**e**) 2.5 ng/ml ciprofloxacin, and (**f**) 1.25 μg/ml ampicillin. Time course measurements of the optical density at 600 nm over 12 h were recorded. Cells were exposed to the antibiotics from the onset of growth. The averages of biological triplicates are shown, and the error bars (shown unless smaller than icons) represent the standard deviations of the mean.

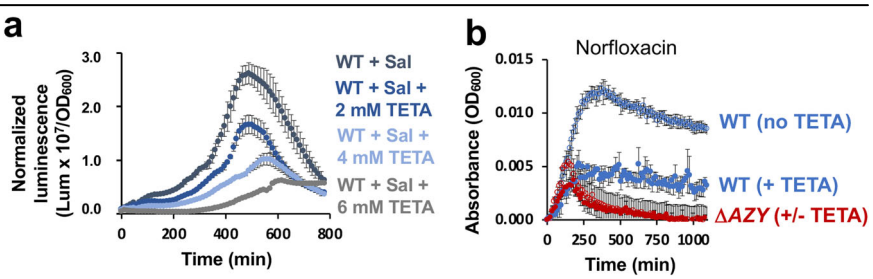

Fig. 5 | Copper import by the AZY proteins is essential for activation of the *mar* operon and for antibiotic resistance. a Cultures of WT cells expressing the luciferase reporter gene fused to the *mar* operator were cultured in the presence of the *mar* operon inducer salicylic acid (2.5 mM) and in the absence or presence of the indicated concentrations of the copper chelator TETA. The averages of biological triplicates are shown, and the error bars (shown unless smaller than icons) represent the standard deviations of the mean. **b** Cultures of WT and Δ*AZY* cells (blue and red curves, respectively) were grown in M9 minimal media in the presence of 62.5 ng/ml norfloxacin, and in the absence (open circles) or presence (full circles) of the copper chelator TETA (2 mM). The experiments are the means of biological triplicates, and the error bars (shown unless smaller than icons) represent the standard deviations of the mean.

(~4%), including that of *M. trichosporium* OB3B CopD[29], include a cytochrome cbb_3 domain linked to a C-terminal domain that resembles Sco1 (44% similarity) or thioredoxin-like proteins[39].

To determine the prevalence of the AZY operon arrangement, we performed an extensive genomic neighborhood analysis of the 5804 proteobacterial CopD-encoding genes included in the SSN analysis. In the 27 common operon types (Supplementary Fig. 11, Fig. 6d) a majority of *copD* genes are found near *copC* (~70%), again consistent with the enhancement of YebZ activity by YobA (Fig. 1d). In ~45% of these operons, *copD* also neighbors genes encoding copper resistance proteins (CopABCD, CopABCDRS, CusABCDEF) or those encoding proteins implicated in copper import and/or delivery pathways (PCu_AC, YcnI, TonB-dependent and ABC transporters, copper ATPases). In addition, many genes near *copD* and *cop* operons encode DUF proteins, including DUF2511, which corresponds to YebY[23], and is present in ~700 operons (17%), including in *Shigella boydii*, *Shigella dysenteriae*, *Salmonella enterica*, *Enterobacter*

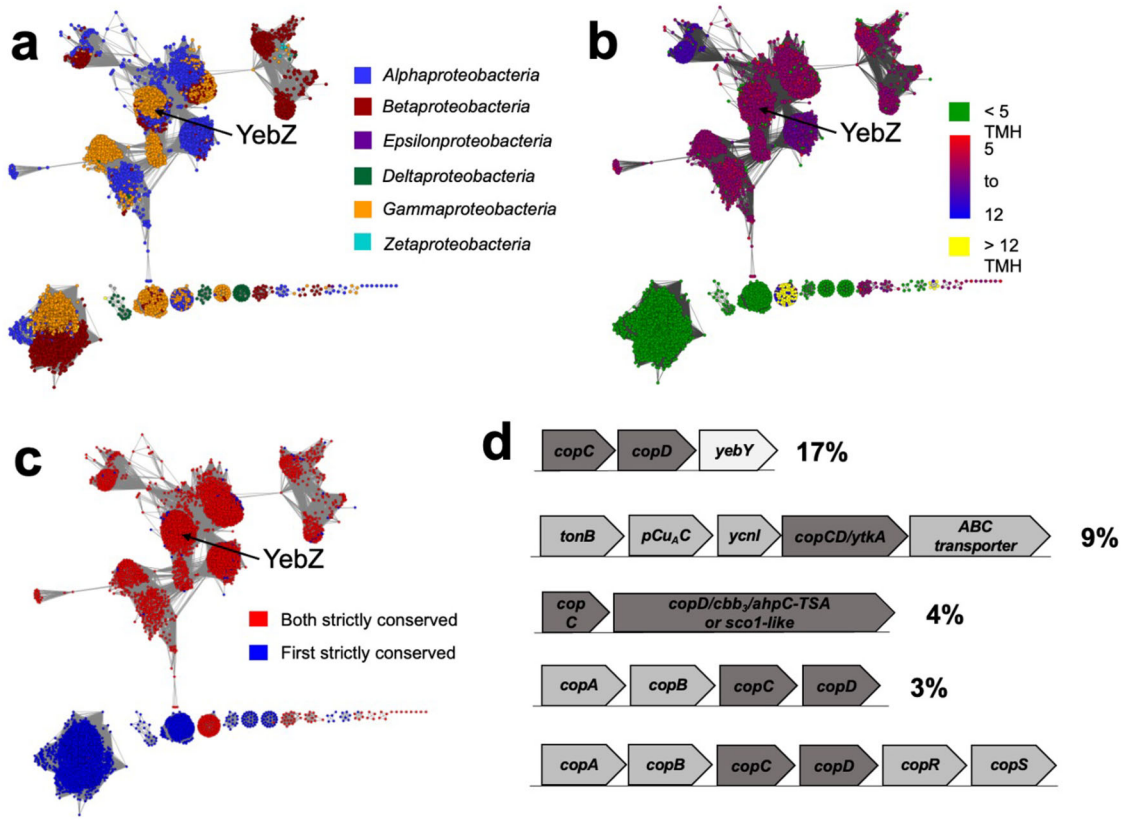

Fig. 6 | Copper import for antibiotic resistance may be a widespread mechanism in bacteria. CopD sequence similarity networks are colored by (**a**) genetic order, (**b**) number of predicted transmembrane helices, and (**c**) strict conservation of the two histidine residues implicated in copper uptake by YebZ. Sequences are clustered in representative nodes at 100% sequence identity using an E-value cutoff of 1E-20. **d** Most common genome neighborhoods of the CopD family, with the genes encoding *copD* and *copC* in dark gray. Percent of total *copD* genes in each neighborhood are indicated.

cloacae, and *Klebsiella pneumoniae*. Thus, copper uptake by the AZY proteins may modulate antibiotic resistance in a wide range of bacteria, including pathogenic strains.

Discussion

While eukaryotes and prokaryotes employ similar copper-specific efflux pumps to avert the toxic effects of copper overload[7,8], specific copper importers have been described in extensive detail only in eukaryotes[7], and the identity of equivalent prokaryotic systems remains elusive. In prokaryotes, the uptake of other transition metal ions into the cytoplasm is mediated by dedicated ABC import systems[40,41]. While outer membrane TonB-dependent transporters can specifically import copper to the periplasm[42,43], a copper-importing ABC transporter has not yet been identified in any species. Thus, the prevailing consensus has been that, with a few exceptions[15,16,25,26,32], most prokaryotes lack a specific import system that delivers copper to the cytoplasm. Contrary to this assumption, we show here that the *E. coli* AZY proteins comprise a widespread copper-specific uptake system. While dominant under the conditions tested, secondary mechanisms of cytoplasmic copper uptake likely exist as well, given the residual copper uptake in the Δ*AZY* strain (Fig. 1a). Importantly, the AZY system plays a key role in regulating multiple antibiotic resistance by providing copper for activation of the *mar* pathway. As such, our data provide an updated model for copper delivery to the cytoplasm, and how this copper is utilized in bacterial antibiotic resistance (Fig. 7). Initially, copper crosses the outer membrane and enters the periplasm through porins[9] or chalkophore uptake systems[10]. Once in the periplasm, copper is bound by YobA[23]. It can then be transferred to membrane embedded cuproenzymes such as NDH-2[23], which may serve as a cytoplasmic copper source under antibiotic stress[20]. Periplasmic copper is also delivered to the cytoplasm by the concerted

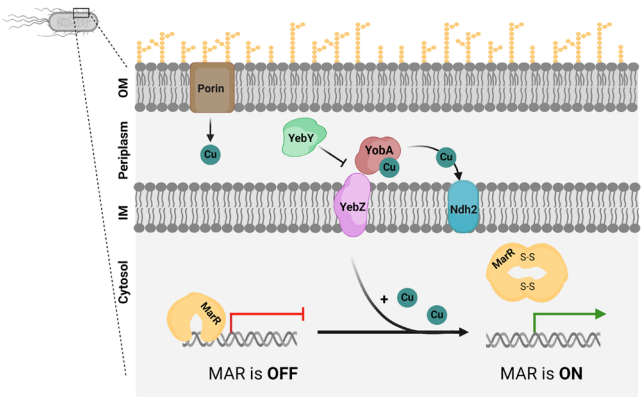

Fig. 7 | Updated model for AZY-mediating copper signaling in *mar* pathway in *E. coli*. Copper enters the cell through extracellular porins or chalkophore-mediated pathways. Once in the periplasm, copper can be trafficked by YobA to deliver copper to the inner membrane transporter YebZ or inner membrane enzymes like NDH-2, which is likely a source of cytoplasmic copper under antibiotic or oxidative stress. Once copper is in the cytoplasm, it can be utilized by MarR to trigger activation of the *mar* pathway, thus leading to multidrug antibiotic resistance. Figure created with BioRender.com.

action of YebZ and YobA where it oxidizes MarR, leading to derepression of the *mar* operon and multidrug resistance[20,22]. At high copper concentrations, YebY may function as a safety valve, preventing toxic copper overload by inhibiting the import activity of YebZ and YobA. Elucidation of this missing link between copper and antibiotic resistance will impact future strategies to combat multidrug resistance.

Methods

Bacterial strains and plasmids for Δ*AZY* knockout

Unless otherwise stated, the *E. coli* strain BW25113, the parental strain of the Keio collection[44], was used in all experiments. The widespread use of this strain and its single-deletion derivatives facilitates direct comparisons between different studies. This strain was also used for generation of the Δ*AZY* strain which lacks the entire *yobA-yebZ-yebY* operon, using the method of Datsenko et al. [45]. We removed the entire AZY operon from the *E. coli* chromosome and subsequently removed the kanamycin cassette used for selection, generating a clean deletion (strain Δ*AZY*). Deletion of the genes encoding the AZY proteins and absence of off-target mutations was verified by PCR and whole genome sequencing. To generate the plasmid $_{p}$*copA-Lux*, the genomic region corresponding to the promoter of *copA* (nucleotide positions 511354–511573) was amplified from a single colony of *E. coli* MG1655 using standard PCR. Using restriction free cloning, the amplicon was then inserted into the $_{p}$*PL2lux* plasmid[46] upstream of the *luxCDABE* operon. To generate the plasmid $_{p}$*marX-Lux*, the genomic region upstream of the *mar* operon (nucleotide positions 1618941-16191200) was amplified from a single colony of *E. coli* MG1655 using standard PCR. This region stretches from the promoter of *marC* to the ATG site of *marR* and includes all the known regulatory elements of the *mar* operon: the marbox, the MarR binding site (*marO*), and the *marR* promoter. This amplicon was inserted into plasmid $_{p}$*PL2lux* upstream of the *luxCDABE* operon as described above.

Growth assays

Unless otherwise stated, for all luciferase activity measurements, cells were cultured in M9 minimal media supplemented with 0.5% glycerol and 0.1% tryptone. Cells were transformed with either the promoter-less Lux plasmid $_{p}$*PL2lux* or with plasmids $_{p}$*copA-Lux* or $_{p}$*marX-Lux* described above. Cultures (150 µL) were diluted to an OD_{600} of 0.01 and grown in a covered 96-well plate at 37 °C in an automated plate reader (InfinitePro 200, Tecan). The OD_{600} and luminescence were measured continuously. All experiments were performed in biological triplicates with at least three technical replicates each.

For growth in the presence of external stressors, cultures were grown in M9 minimal media supplemented with 0.5% glycerol and 0.1% tryptone for 3 h and then diluted to an OD_{600} of 0.01. Stressors (ethanol, sodium dodecyl sulfate, or sodium cholate) or antibiotics were added as indicated. Cultures (150 µL) were grown in a covered 96-well transparent plate an automated plate reader at 37 °C for 12 h. The OD_{600} was measured continuously, and all experiments were performed in biological triplicates with at least three technical replicates each.

Overexpression of AZY operon proteins

The codon-optimized genes for YebZ (JGI Gene ID 637001825, Meta Draft AC_000091.cds1796.1926305. 1925433), YebY (JGI Gene ID 637001824, Meta Draft AC_000091.cds1795.1925420. 1925079), and YobA (JGI Gene ID 637001826, Meta Draft AC_000091.cds1797.1926683. 1926309) were obtained from GenScript and were cloned into pET-22b(+), pET-21b(+), and pCDF-Duet 1 plasmids using "EZcutter" restriction sites. Single point mutants of YebZ in pET-22b(+) vectors were generated via site directed mutagenesis and purchased through GenScript. HmtA from *Pseudomonas aeruginosa* Q9I147 in a pBAD vector was generated as described previously[32]. Attempts to overexpress the AZY operon proteins or YebZ in *E. coli* BL21 cells were unsuccessful, likely due to the well-documented challenges of expressing membrane proteins. Therefore, we used *E. coli* C41(DE3), a strain specifically developed to overcome such obstacles. The plasmids were transformed into OverExpress™ C41(DE3) Star cells (New England Biosciences) via electroporation, and positive transformants were selected on LB medium containing either ampicillin (50 µg/mL, DOT Scientific) or spectinomycin (70 µg/mL, Research Products Inc.). Single colonies were resuspended in 5 mL of LB media, allowed to grow overnight at 37 °C and 200 rpm, and glycerol stocks were prepared for in vivo metal transport assays.

In vivo metal transport assays

Cultures were grown in the absence of metals at 200 rpm and 37 °C to an OD_{600} of 1.0 in LB medium supplemented with 50 µg/mL ampicillin, followed by induction with 100 µM IPTG. After incubation for 2.5 h, the OD_{600} values of the cultures were measured, and cell aliquots were placed on ice for 30 min before centrifugation at 4000 g for 5 min. Cells were washed with 50 mM potassium phosphate (pH 7.5) and 2 mM $MgCl_2$ and resuspended in the same buffer to an OD_{600} of 2.5. After 10 min recovery in the presence of 0.2% glucose at 200 rpm and 37 °C, metals were added at various concentrations. Metals were freshly prepared as 0.1 M stock solutions of $ZnCl_2$, $FeSO_4$, $CoCl_2$, and $CuSO_4$ in trace metal free tubes using MilliQ water. After 30 min, a 2–5 mL sample was withdrawn, centrifuged at 4000 g for 5 min, washed with 50 mM potassium phosphate (pH 7.5) and 10 mM EDTA, and centrifuged again for a total of three times. Cell pellets were resuspended in 5 mL of MilliQ water, and metal contents were measured directly by inductively coupled plasma mass spectrometry (ICP-MS, Thermo iCAP Q, Northwestern Quantitiative Biological Imaging Facility). Nonspecific metal uptake was accounted for by normalizing the data to the background metal content in C41(DE3) cells expressing a control plasmid (pET or pCDF-Duet). ICP-MS samples were prepared in 5% trace metal free nitric acid and 1% trace metal free hydrogen peroxide with 5 ppb indium, lithium, scandium, and yttrium standards (Inorganic Ventures). The concentrations of iron, cobalt, nickel, copper, and zinc were measured using the NWU-16 (Inorganic Ventures) multielement standard.

AlphaFold modeling of YebZ and YobA

All AlphaFold modeling was executed on Jupyter notebooks via Google Colaboratory. Multiple sequence alignments (MSAs) for each modeled sequence were generated using the MMseqs2-based routine implemented in ColabFold, in which sequences were searched in three iterations against the consensus sequences of UniRef30. Hits were accepted with an E-value lower than 0.1. For each hit, the respective UniRef30 cluster member was realigned to the profile generated in the last iterative search, filtered such that no cluster had a higher maximum sequence identity than 95%, and added to the MSA. AlphaFold Multimer was implemented using MMseqs2 to search against PDB70 cluster representatives to generate 20 target templates. Models of YebZ and YobA were then generated through a paired alignment and modification of the residue index to generate the top five most likely structures to be adopted by the sequence as determined by the pLDDT. Since this complex is heterooligomeric, a separate MSA was generated for each component and paired using the pLDDT to determine local structure confidence and pTMscore to determine optimal complex formation. All models were manually inspected and compared. The sequence logo for YebZ was calculated with Jalview and MAFFT.

Identification and network analysis of CopD homologs in bacterial genomes

All gram-negative protein sequences matching the CopD PFAM profile hidden Markov Model (HMM) (PF05245) and associated metadata were obtained from the JGI-IMG database (https://img.jgi.doe.gov/, April 21, 2021), comprising ~50,000 total sequences. Similar to previous analyses[47], initial SSNs were generated using the enzyme function initiative-enzyme similarity tool (EFI-EST) and trimmed on the basis of length with a cutoff to remove sequences with fewer than 100 or greater than 750 residues. An E-value cut off of 1E-20 was used, and sequences with 100% identity were clustered into single nodes, decreasing overrepresented sequences and yielding a final network with 5804 representative nodes. The EFI-EST representative nodes were then correlated with the input list of proteins, and the amino acid sequences for only the representative nodes were retrieved. A tab-delimited text file identifying characteristics of interest for each node was overlaid onto the network using Cytoscape-3.5.1. The phylum, additional domain co-annotations, and sequence length were obtained from exported JGI metadata for each gene. Using a previously created sequence logo generated using MAFFT, conservation information was added to the SSN metadata and visualized.

Genomic clustering of CopD neighborhoods

Metadata for all genes within five ORFs of *copD* (i.e., ±5 genes upstream and downstream) that occur in > 2.0% of the CopD neighborhoods were collected. Neighboring genes were classified by annotated PFAM and TIGRFAM profile HMMs, as were any additional fusion domains and the presence of predicted and annotated metal binding sites. These traits and the CopDs associated with them were subjected to hierarchical clustering using the R package "prettyClusters"[48]. Briefly, clustering was calculated in R using the Manhattan method (absolute distance) in the *dist* function to calculate the distance matrix. Clustering was determined using the Ward.D2 method in the *hclust* function. To generate dendrograms and a heat map from the hierarchical clustering data, the heatmap.2 function in gplots was used. Clustered sets of traits were determined using a cluster cutoff to establish 27 primary operon groups. Neighborhood architectures were visually inspected to identify protein functions, and any genes likely to be unrelated to copper homeostasis were eliminated. Finally, 3-5 randomly selected *copDs* from each of the largest 27 operon families were checked to visually confirm the clustering results.

Statistics and reproducibility

All statistical analyses were performed using GraphPad Prism version 10.1.1. Comparisons between two groups were conducted by an unpaired, two-tailed student's t-test, and respective p values are reported in the figure captions. For data that contain comparisons between more than two groups, one-way or two-way ANOVA followed by Tukey-Kramer's multiple comparisons test were performed, with *p*-value ranges listed in the figure captions. Time course experiments are presented as mean ± standard deviations of the mean (SEM), and if the SEM is smaller than the mean, this is noted in the figure caption. Each group of measurements contains at least three biological and three technical replicates, with the specific number listed in the caption for each experiment. Each biological replicate represents an independent sample from a separate bacterial growth to ensure reproducibility. For the bioinformatics analysis, the sequence similarity networks are displayed with representative nodes for CopD family members to prevent over-biasing important features, and these sequences were utilized to prevent overrepresentation in sequence alignments.

Reporting summary

Further information on research design is available in the Nature Portfolio Reporting Summary linked to this article.

Data availability

All data generated or analyzed during this study are included in the published article, Supplementary Information, or Supplementary Data files, including numerical source data for Figs. 1–5, and bioinformatics analysis for Fig. 6. All other data are available from the corresponding authors upon reasonable request.

Received: 24 September 2024; Accepted: 4 March 2025;
Published online: 19 March 2025

References

1. Tsang, T., Davis, C. I. & Brady, D. C. Copper biology. *Curr. Biol.* **31**, R421–R427 (2021).
2. Solomon, E. I. et al. Copper active sites in biology. *Chem. Rev.* **114**, 3659–3853 (2014).
3. Han, J. Copper trafficking systems in cells: insights into coordination chemistry and toxicity. *Dalton Trans* **52**, 15277–15296 (2023).
4. Rohaun, S. K. & Imlay, J. A. The vulnerability of radical SAM enzymes to oxidants and soft metals. *Redox Biol* **57**, 102495 (2022).
5. Tsvetkov, P. et al. Copper induces cell death by targeting lipoylated TCA cycle proteins. *Science* **375**, 1254–1261 (2022).
6. Novoa-Aponte, L. & Argüello, J. M. Unique underlying principles shaping copper homeostasis networks. *J. Biol. Inorg. Chem.* **27**, 509–528 (2022).
7. Lutsenko, S. Dynamic and cell-specific transport networks for intracellular copper ions. *J. Cell Sci*. **134**, jcs240523 (2021).
8. Andrei, A. et al. Cu homeostasis in bacteria: the ins and outs. *Membranes* **10**, 242 (2020).
9. Stewart, L. J. et al. Handling of nutrient copper in the bacterial envelope. *Metallomics* **11**, 50–63 (2019).
10. Kenney, G. E. & Rosenzweig, A. C. Chalkophores. *Annu. Rev. Biochem.* **87**, 645–676 (2018).
11. Argüello, J. M., Raimunda, D. & Padilla-Benavides, T. Mechanisms of copper homeostasis in bacteria. *Front. Cell. Infect. Microbiol.* **3**, 14 (2013).
12. González-Guerrero, M., Raimunda, D., Cheng, X. & Argüello, J. M. Distinct functional roles of homologous Cu+ efflux ATPases in *Pseudomonas aeruginosa*. *Mol. Microbiol.* **78**, 1246–1258 (2010).
13. Hassani, B. K., Astier, C., Nitschke, W. & Ouchane, S. CtpA, a copper-translocating P-type ATPase involved in the biogenesis of multiple copper-requiring enzymes. *J. Biol. Chem.* **285**, 19330–19337 (2010).
14. Osman, D. et al. The copper supply pathway to a *Salmonella* Cu,Zn-superoxide dismutase (SodCII) involves P1B-type ATPase copper efflux and periplasmic CueP. *Mol. Microbiol.* **87**, 466–477 (2013).
15. Ekici, S., Yang, H., Koch, H. G. & Daldal, F. Novel transporter required for biogenesis of *cbb*3-type cytochrome *c* oxidase in *Rhodobacter capsulatus*. *mBio* **3**, e00293–e00311 (2012).
16. Quintana, J., Novoa-Aponte, L. & Argüello, J. M. Copper homeostasis networks in the bacterium *Pseudomonas aeruginosa*. *J Biol Chem* **292**, 15691–15704 (2017).
17. Philips, S. J. et al. Allosteric transcriptional regulation via changes in the overall topology of the core promoter. *Science* **349**, 877–881 (2015).
18. Martin, R. G. & Rosner, J. L. Binding of purified multiple antibiotic-resistance repressor protein (MarR) to mar operator sequences. *Proc. Natl. Acad. Sci. USA* **92**, 5456–5460 (1995).
19. Alekshun, M. N. & Levy, S. B. Regulation of chromosomally mediated multiple antibiotic resistance: the *mar* regulon. *Antimicrob. Agents Chemother.* **41**, 2067–2075 (1997).
20. Hao, Z. et al. The multiple antibiotic resistance regulator MarR is a copper sensor in *Escherichia coli*. *Nat. Chem. Biol.* **10**, 21–28 (2014).
21. Cohen, S. P., Yan, W. & Levy, S. B. A multidrug resistance regulatory chromosomal locus is widespread among enteric bacteria. *J. Infect. Dis.* **168**, 484–488 (1993).
22. Sharma, P. et al. The multiple antibiotic resistance operon of enteric bacteria controls DNA repair and outer membrane integrity. *Nat. Commun.* **8**, 1444 (2017).
23. Hadley, R. C. et al. The copper-linked *Escherichia coli* AZY operon: Structure, metal binding, and a possible physiological role in copper delivery. *J. Biol. Chem.* **298**, 101445 (2022).
24. Rensing, C. & Grass, G. *Escherichia coli* mechanisms of copper homeostasis in a changing environment. *FEMS Microbiol. Rev.* **27**, 197–213 (2003).
25. Chillappagari, S., Miethke, M., Trip, H., Kuipers, O. P. & Marahiel, M. A. Copper acquisition is mediated by YcnJ and regulated by YcnK and CsoR in *Bacillus subtilis*. *J. Bacteriol.* **191**, 2362–2370 (2009).
26. Hirooka, K., Edahiro, T., Kimura, K. & Fujita, Y. Direct and indirect regulation of the *ycnKJI* operon involved in copper uptake through two transcriptional repressors, YcnK and CsoR, in *Bacillus subtilis*. *J. Bacteriol.* **194**, 5675–5687 (2012).
27. Cha, J. S. & Cooksey, D. A. Copper hypersensitivity and uptake in *Pseudomonas syringae* containing cloned components of the copper resistance operon. *Appl. Environ. Microbiol.* **59**, 1671–1674 (1993).
28. Cooksey, D. A. Molecular mechanisms of copper resistance and accumulation in bacteria. *FEMS Microbiol. Rev.* **14**, 381–386 (1994).
29. Kenney, G. E., Sadek, M. & Rosenzweig, A. C. Copper-responsive gene expression in the methanotroph *Methylosinus trichosporium* OB3b. *Metallomics* **8**, 931–940 (2016).

30. Pozzi, R. et al. Distinct mechanisms contribute to immunity in the lantibiotic NAI-107 producer strain *Microbispora* ATCC PTA-5024. *Environ. Microbiol.* **18**, 118–132 (2016).
31. Outten, F. W., Outten, C. E., Hale, J. & O'Halloran, T. V. Transcriptional activation of an *Escherichia coli* copper efflux regulon by the chromosomal MerR homologue, cueR. *J. Biol. Chem.* **275**, 31024–31029 (2000).
32. Lewinson, O., Lee, A. T. & Rees, D. C. A P-type ATPase importer that discriminates between essential and toxic transition metals. *Proc. Natl. Acad. Sci. USA* **106**, 4677–4682 (2009).
33. Evans, R. et al. Protein complex prediction with AlphaFold-Multimer. *bioRxiv*, 2021.10.04.463034 (2022).
34. Cohen, S. P., Levy, S. B., Foulds, J. & Rosner, J. L. Salicylate induction of antibiotic resistance in *Escherichia coli*: activation of the *mar* operon and a *mar*-independent pathway. *J. Bacteriol.* **175**, 7856–7862 (1993).
35. Pham, T. D. M., Ziora, Z. M. & Blaskovich, M. A. T. Quinolone antibiotics. *MedChemComm* **10**, 1719–1739 (2019).
36. Lima, L. M., da Silva, B. N. M., Barbosa, G. & Barreiro, E. J. β-lactam antibiotics: An overview from a medicinal chemistry perspective. *Eur. J. Med. Chem.* **208**, 112829 (2020).
37. Kohanski, M. A., Dwyer, D. J., Hayete, B., Lawrence, C. A. & Collins, J. J. A common mechanism of cellular death induced by bactericidal antibiotics. *Cell* **130**, 797–810 (2007).
38. Rudilla, H. et al. New and old tools to evaluate new antimicrobial peptides. *AIMS Microbiol* **4**, 522–540 (2018).
39. Horng, Y.-C. et al. Human Sco1 and Sco2 function as copper-binding proteins. *J. Biol. Chem.* **280**, 34113–34122 (2005).
40. Kuznetsova, A. et al. Titratable transmembrane residues and a hydrophobic plug are essential for manganese import via the *Bacillus anthracis* ABC transporter MntBC-A. *J. Biol. Chem.* **297**, 101087 (2021).
41. Patzer, S. I. & Hantke, K. The ZnuABC high-affinity zinc uptake system and its regulator Zur in *Escherichia coli*. *Mol. Microbiol.* **28**, 1199–1210 (1998).
42. Dassama, L. M., Kenney, G. E., Ro, S. Y., Zielazinski, E. L. & Rosenzweig, A. C. Methanobactin transport machinery. *Proc. Natl. Acad. Sci. USA* **113**, 13027–13032 (2016).
43. Bhamidimarri, S. P. et al. Acquisition of ionic copper by the bacterial outer membrane protein OprC through a novel binding site. *PLoS Biol* **19**, e3001446 (2021).
44. Baba, T. et al. Construction of *Escherichia coli* K-12 in-frame, single-gene knockout mutants: the Keio collection. *Mol. Syst. Biol.* **2**, 2006.0008 (2006).
45. Datsenko, K. A. & Wanner, B. L. One-step inactivation of chromosomal genes in *Escherichia coli* K-12 using PCR products. *Proc. Natl. Acad. Sci. USA* **97**, 6640–6645 (2000).
46. Haber, A. et al. L-glutamine induces expression of *Listeria monocytogenes* virulence genes. *PLoS Pathog* **13**, e1006161 (2017).
47. Lawton, T. J., Kenney, G. E., Hurley, J. D. & Rosenzweig, A. C. The CopC family: structural and bioinformatic insights into a diverse group of periplasmic copper binding proteins. *Biochemistry* **55**, 2278–2290 (2016).
48. Kenney, G. E. _prettyClusters: Exploring and Classifying Genomic Neighborhoods Using IMG-Like Data_. R package version 0.2.3. (2023).

Acknowledgements

This work was supported by NSF-BSF MCB grant 1938715 (A.C.R., O.L.). C.D.P. was supported in part by NIH grant T32GM008382. Research in the Lewinson lab is supported in part by the Rappaport Institute for Biomedical Research. ICP-MS analysis was performed at the Quantitative Bio-element Imaging Center at Northwestern University, supported by NASA Ames Research Center Grant NNA04CC36G.

Author contributions

A.C.R. and O.L. conceptualized the work, and C.D.P., Y.G., N.L.L. designed experiments. C.D.P., Y.G., and N.L.L. performed experiments, analyzed data, and prepared figures. C.D.P., Y.G., N.L.L., A.C.R., and O.L. contributed to writing and editing the manuscript.

Competing interests

The authors declare no competing interests.

Additional information

Supplementary information The online version contains supplementary material available at https://doi.org/10.1038/s42003-025-07884-5.

Correspondence and requests for materials should be addressed to Oded Lewinson or Amy C. Rosenzweig.

Peer review information *Communications Biology* thanks Junqi Xu, Michael Johnson, and the other, anonymous, reviewer for their contribution to the peer review of this work. Primary Handling Editors: Ranjana Pathania and Tobias Goris.